Investigation of quartz ESR residual signals in the last glacial and early Holocene fluvial deposits from the Lower Rhine

Marcus Richter[1] and Sumiko Tsukamoto[1]

[1]Leibniz Institute for Applied Geophysics (LIAG), Stilleweg 2, 30655 Hanover, Germany

Correspondence: Marcus Richter (Marcus.Richter@leibniz-liag.de)

Abstract. In this study, we examined the residual doses of the quartz electron spin resonance (ESR) signals from eight young fluvial sediments with known luminescence ages from the lower Rhine terraces. The single aliquot regenerative (SAR) protocol was applied to obtain the residual doses for both the Aluminium (Al) and Titanium (Ti) impurity centres. We show that all of the fluvial samples carry a significant amount of residual dose with a mean value of ~~1320~~ 1270 ± 120 Gy for the Al centre (including the unbleachable signal ~~part~~component), ~~610~~ 591 ± ~~60~~ 53 Gy for the lithium-compensated Ti centre (Ti-Li), ~~180~~ 170 ± 21~~0~~ Gy for the hydrogen- compensated Ti centre (Ti-H), and 453~~470~~ ± ~~40~~ 42 Gy for the signal originated from both the Ti-Li and Ti-H centres (termed Ti-mix). To test the accuracy of the ESR SAR protocol, a dose recovery test was conducted and this confirmed the validity of the Ti-Li and Ti-mix signal results. The Al centre shows a dose recovery ratio of 1.74 ± 0.16~~, probably due to a sensitivity change by the thermal treatment in the SAR procedure~~, whereas the Ti-H signal shows a ratio of 0.56 ± 0.17, suggesting that the rate of signal production per unit dose changed for these signals after the thermal annealing. ~~. Hence, it can be assumed that the residual dose for the Al centre is overestimated whereas it is underestimated for the Ti-H signal.~~ Nevertheless ~~The~~all fluvial sediments investigated in this study carry a significant residual dose. Our result suggests that more direct comparisons between luminescence and ESR equivalent doses should be carried out, and if necessary, the subtraction of residual dose obtained from the difference is essential to obtain reliable ESR ages.

1 Introduction

When sedimentary quartz was first investigated for electron spin resonance (ESR) dating 35 years ago by Yokoyama et al. (1985) a bleaching test was performed and an optically unbleachable residual signal for the Al centre was detected. Moreover "zero age" samples were investigated, residual signals were detected, and subsequently subtracted from the natural signal intensity to calculate the equivalent dose (D_e). This procedure led to ESR ages which were in good agreement with expected ages. Over the years, several bleaching experiments on quartz ESR signals were conducted and varying proportions of bleachable and unbleachable signal intensities for the Al centre were reported

Formatiert: Nummerierung: Fortlaufend

Formatiert: Rechts: 0,1 cm

Formatiert: Schriftart: Times New Roman, Nicht Kursiv

(e.g. Toyoda et al., 2000; Voinchet et al., 2003; Rink et al., 2007; Tsukamoto et al., 2018; Beerten et al., 2020). The Ti centre instead showed a better but varying optical bleachability depending on the monovalent charge compensator: the Ti-Na centre and the Ti-H centre were fully bleached within 24 hours of artificial optical bleaching using a halogen lamp, whereas the Ti-Li centre was bleached within 72 to 168 hours (Toyoda et al., 2000). Investigations of different samples revealed a significant variability in bleaching kinetics for both the Ti-Li and the Ti-H signal (e.g. Tissoux et al., 2007; Duval et al., 2017). The Ti centre is believed to be fully bleachable by sunlight exposure (e.g. Toyoda et al., 2000; Tissoux et al., 2007). So far very few studies have reported residual doses of the quartz ESR signals from young or modern analogue samples, which could be directly comparable with the quartz OSL D_e values. Beerten et al. (2006) found a total of 55 Gy (Ti-Li) for the youngest sample in a aeolian sedimentary profile and see this as a strong indicator of an unbleachable or unbleached residual dose. Tsukamoto et al. (2017) used modern aeolian quartz samples, whose optically stimulated luminescence (OSL) signal is well bleached, to investigate the bleachability of the ESR signals. They found large and varying residual doses for both the Al and Ti centres; from 130 to larger than 1700 Gy for the Al centre (including the unbleachable signal ~~part~~component) and from 60 to 460 Gy for the Ti centre. They thus emphasised the importance of subtracting the residual dose, not only for the Al centre but also for the Ti centre. Timar-Gabor et al. (2020) measured the residual dose of aeolian samples from Australia and Ukraine, which have reported OSL D_e values. For all samples, the ESR residual doses were found to be significantly larger than the OSL D_e, with the Al centre (also with unbleachable signal ~~part~~component) ranging from 480 to 700 Gy and the Ti centre ranging 100 to 580 Gy, highlighting the necessity of performing a residual dose subtraction. Although studies were done on dating fluvial sediments using ESR (e.g. Yokoyama et al., 1985; Laurent et al., 1998; Bahain et al., 2007; Tissoux et al., 2007, 2008; Duval et al., 2015, 2020; Bartz et al., 2018; Voinchet et al., 2019; del Val et al., 2019) the potential effect of the residual signals before deposition in both the Al centre and Ti centre have not been well investigated. Voinchet et al. (2015) introduced a bleaching index for various fluvial and aeolian sediment samples and very small residual dose of 4-28 Gy, after subtracting the unbleachable signal of the Al centre have been reported. Toyoda et al. (2000) conducted a comparison of the signal bleachability derived from multiple signals. Based on the result, they reported quartz ESR intensities from multiple centres with different bleachability. An agreement of the ages can confirm that the signals were well bleached before deposition. Since then this so called "multiple centres" approach has been applied in several studies (e.g Duval et al., 2015, 2017; Bartz et al., 2018, 2020). Similar comparison was also conducted between the quartz ESR ages and feldspar post-IR IRSL or quartz thermally transferred (TT-) OSL ages (Bartz et al., 2019, 2020).

Another important issue, which affects the accuracy of ESR dating is the ability of the measurement protocol to recover a known dose (Murray and Wintle, 2003). Previously, ESR dose recovery tests have been conducted by Beerten et al. (2008) on quartz derived from dune sands and Asagoe et al. (2011), who used quartz from tephra samples. Unfortunately, both studies use an intensive thermal treatment (annealing) of the sample to erase the natural

Formatiert: Tiefgestellt

Formatiert: Schriftart: Times New Roman, Nicht Kursiv

Formatiert: Schriftart: Times New Roman, Nicht Kursiv

signal before artificial irradiation, which reduces the significance of the test. Tsukamoto et al. (2017) applied a SAR-SARA (single aliquot regeneration and added dose; Mejdahl and Bøtter-Jensen (1994)) procedure for unheated modern sediments, and used a slope between the added dose on top of the natural dose and the measured dose as a surrogate for the dose recovery ratio (Kars et al., 2014). A similar method was also adopted by Toyoda et al. (2009) and Fang and Grün (2020) who plotted the relationship between the added dose on natural aliquots and the increase in the apparent dose.

This study aims to investigate the size of the residual doses for the quartz Al and Ti centres in fluvial sediments using 8 samples with known OSL ages (Lauer et al., 2011). In this study, we define the residual dose as the ESR D_e values minus the OSL D_e of the same sample, and this include both bleachable and unbleachable ~~parts~~ components of the Al centre. These young sediments are investigated using the ESR SAR protocol and its performance is monitored by conducting dose recovery tests.

Formatiert: Schriftart: Times New Roman, Nicht Kursiv

Formatiert: Schriftart: Times New Roman, Nicht Kursiv

2 Samples

Fluvial sediments from Lauer et al. (2011) are from five gravel pits on either side of the Lower terraces of the Rhine (Frechen, 1992) covering a clearance of 90 km from Niederkassel to Rheinberg, North Rhine-Westphalia, were used in this study. All sediments originated from the younger Lower terrace of the Rhine River. A brief description of the samples is given in Table 1 and a detailed description of the sedimentary environment is given in Lauer et al. (2011). Previous work from Lauer et al. (2011) provides OSL D_e using SAR protocol in the range of several tens of Gray (cf. Table 2). They used IR-stimulated and yellow-stimulated luminescence signals of potassium-rich feldspar as well as OSL of quartz to date a total of 11 samples. Mean quartz OSL D_e-values are ranging from 14.8 ± 0.3 Gy to 33.3 ± 1.4 Gy with dose rates in the range of 1.48 ± 0.15 Gy/ka to 2.~~57~~ 41 ± 0.~~27~~ 18 Gy/ka. The mean OSL ages range from 8.6 ± 0.5 ka to 16.0 ± 1.3 ka (cf. Table 3). Thus, the sediments are Holocene or late Pleistocene age rendering them to be treated as young samples for ESR residual measurements. All samples show the Al and Ti centres, but three samples (ALH-I, ALH-II and MHT-I~~II~~) showed a broad and strong, overlapping signal, presumably arising from paramagnetic Mn^{2+} and Fe^{3+} impurities. Eventually, eight samples of a grain size ranging 100-250 microns were used to conduct ESR measurements. These are exactly the same samples that (Lauer et al., 2011) used. No additional preparation steps were taken.

Formatiert: Schriftart: Times New Roman, Nicht Kursiv

Formatiert: Schriftart: Times New Roman, Nicht Kursiv

3 ESR measurements

A Bruker ELEXSYS E500 X-band ESR spectrometer with a variable temperature controller was used to run all measurements. The temperature inside the ER4119HS cavity was kept at 100 K through the evaporation of liquid nitrogen. The measurement settings for the detection of the Al centre $[AlO_4]^0$ were: 335 ± 15 mT scanned magnetic field, modulation amplitude 0.1 mT, modulation frequency 100 kHz, 40 ms conversion time and 122.9 s sweep time and 3-5 scans. For the Ti centre $[TiO_4/M^+]^0$ the settings were: 350 ± 5 mT scanned magnetic field, modulation amplification 0.1 mT, modulation frequency 100 kHz, 30 ms conversion time and 61.4 s sweep time and 5-10 scans of the spectra. For all measurements the microwave power was kept at 10 mW and the sample size was 60 mg. The light exposure of the quartz grains within the ESR quartz-glass sample tubes was kept at a minimum during the heating, artificial irradiation and ESR measurements. Furthermore, sample tubes were stored in opaque black plastic bags between measurements. During the measurements, meticulous care was taken to ensure that the sample quantity and sample tube positioning and measurement temperature always remained the same for all measurements. The quality factor (Q) of the cavity was always greater than 8000 during the runs. All the samples were rotated 3 times in the cavity to calculate the mean signal intensity and to take into account the angular dependence of the signal.

As suggested by Toyoda and Falguères (2003) the intensity of the Al centre was taken from the first (g = 2.0185) to the last peak (g = 1.9928), as depicted in Fig. 1A. The overlapping peroxy signal intensity was subtracted eventually by using the ESR signal intensity after annealing (Step 4; see Table 4). The intensity of the Ti centre signals was evaluated from peak-to-baseline or peak-to-peak amplitude following Tissoux et al. (2008); Duval and Guilarte (2015); Duval et al. (2017) (Fig. 1A and 1B). The intensity of the Ti-Li centre was taken from the baseline to the peak at g_3 = 1.913, although this may be affected by Ti-H centre (cf. Tissoux et al., 2008). The intensity of the Ti-H centre was calculated from the g_3 = 1.915 peak to the baseline. Duval and Guilarte (2015) used the peak-to-peak intensity at around g_2 = 1.931 (cf. Fig. 1A and 1B) originating from both Ti-H and Ti-Li centres (referred to called Ti-mix in this study). These three different measurement options for the Ti centre are equivalent to Option D, C, and B of Duval and Guilarte (2015), respectively. An in-house built X-ray irradiator, consisting of a Spellmann XRB401 source, was used for all laboratory irradiations. The X-ray parameters were fixed to 200 kV and 2 mA and the dose rate was calibrated to 0.052 ± 0.004 Gy/s (Tsukamoto et al., ~~submitted).~~2021). For heating and annealing of samples, an in-house built device was used (Oppermann and Tsukamoto, 2015). The dose response curve (DRC) was fitted to a single saturated exponential function using Origin 2017 without any weighting to calculate D_e.

4 Performance tests and equivalent dose

Preheat Plateau test

The ESR SAR protocol (see Table 4), which has been tested and satisfyingly applied in previous studies in regards to the Ti centre (Tsukamoto et al., 2015, 2017, 2018; Richter et al., 2020) was used for all measurements. Prior to

Formatiert: Tiefgestellt

Formatiert: Hochgestellt

Formatiert: Tiefgestellt

Formatiert: Hochgestellt

Formatiert: Hochgestellt

Formatiert: Schriftart: Times New Roman, Nicht Kursiv

D_e measurements a preheat plateau test was carried out to assure only stable signals are used. The sample with the lowest quartz OSL D_e was chosen for this test (RB-II; 14.8 ± 0.3 Gy). Temperatures were set to 160, 180, 200 and 220 °C. Additionally an aliquot without heating treatment was used, which is referred to as 20 °C (room temperature). Heating time was 4 minutes for preheating and 120 minutes for annealing at 300 °C. In a previous study, Tsukamoto et al. (2015) compared 420 °C for 2 minutes and 300 °C for 120 minutes annealing time and found no significant difference in sensitivity change between both temperatures. Artificial irradiation dose steps used were 241 Gy, 963 Gy and 2889 Gy to construct a dose response curve. The results are plotted in Fig. 2A. The D_e value of the Al centre was initially decreased by the preheat at 160 °C, but shows a steady increase in D_e with increasing preheat temperature. At 220 °C no D_e calculation was possible, because all regenerated signal intensities were below the natural. The Ti-Li and Ti-mix signals show a similar pattern in D_e; there was a small decrease from room temperature to 160 °C, but all preheats yielded similar D_e values, albeit a slight increasing trend with increasing temperature was observed. The Ti-H centre showed an opposite trend to the Ti-Li and Ti-mix and showed a decrease in D_e with higher temperatures >180 °C. Eventually, the preheat temperature was set to 160 °C for all of the following measurements because Ti-Li, Ti-H and Ti-mix D_e tend to form a plateau in the region of 160-180 °C preheat temperature. An overview over the DRC's for 160 °C are shown in Fig. 2A, and for each preheat temperature for each one of the ESR centres can be found in the supplement Fig. A1.

Equivalent doses, residual doses and ESR ages

For each ~~of the samples~~sample, one aliquot was used to conduct the D_e measurements. Dose response curves were created using 3 regenerated dose steps with a total dose up to 2889 Gy for all samples except for sample NK-1, NK-2 and ALH-III which were irradiated up to 3022 Gy. The D_e values of the Al centre are in the range of ~~1000~~ 961 to ~~2040~~ 1960 Gy (including the unbleachable signal component). The D_e values of the Ti-Li centre spans from ~~430~~413 to 893~~930~~ Gy. The Ti-mix D_e ranges from 292~~300~~ to 677~~700~~ Gy and the Ti-H D_e goes from ~~120~~ 115 to 292~~300~~ Gy. The mean OSL D_e for each sample was subtracted from the ESR D_e to calculate the residual dose. This led to a residual dose of Al centre in the range of ~~970~~931 to 1930~~2000~~ Gy and with a mean value (± 1 SE) of ~~1320~~1270 ± 120 Gy (including the unbleachable signal component). The Ti-Li centre residual dose goes from 384~~400~~ to 859~~900~~ Gy with a mean of 591~~610~~ ± 53~~60~~ Gy. The Ti-mix residual dose goes from ~~270~~262 to ~~670~~643 Gy with a mean of ~~470~~453 ± ~~40~~ 42 Gy and Ti-H from 95~~100~~ to ~~280~~264 Gy with a mean of 17~~8~~0 ± ~~20~~ 21 Gy. A detailed overview is given in Table 2. Residual doses of the four different ESR signals for all samples is plotted in Fig. 3. A detailed list of ages is given in Table 3. All the ESR ages significantly overestimate the OSL ages. The ages (calculated from the residual dose) are on average ~~650~~ 634 ± ~~60~~ 54 ka for Al centre (including the unbleachable signal component), ~~300~~ 294 ± ~~30~~ 25 ka for the Ti-Li, ~~230~~ 227 ± ~~20~~ 22 ka for the Ti-mix and ~~90~~ 84 ± 10 ka for the Ti-H centre. These residual ages

Formatiert: Schriftart: Times New Roman, Nicht Kursiv
Formatiert: Schriftart: Times New Roman, Nicht Kursiv
Formatiert: Schriftart: Nicht Kursiv
Formatiert: Schriftart: Times New Roman, Nicht Kursiv
Formatiert: Schriftart: Times New Roman, Nicht Kursiv
Formatiert: Schriftart: Times New Roman, Nicht Kursiv
Formatiert: Schriftart: Times New Roman, Nicht Kursiv
Formatiert: Schriftart: Times New Roman, Nicht Kursiv
Formatiert: Schriftart: Times New Roman, Nicht Kursiv
Formatiert: Schriftart: Times New Roman, Nicht Kursiv
Formatiert: Schriftart: Times New Roman, Nicht Kursiv
Formatiert: Schriftart: Times New Roman, Nicht Kursiv
Formatiert: Schriftart: Times New Roman, Nicht Kursiv
Formatiert: Schriftart: Times New Roman, Nicht Kursiv
Formatiert: Schriftart: Times New Roman, Nicht Kursiv
Formatiert: Schriftart: Times New Roman, Nicht Kursiv
Formatiert: Schriftart: Times New Roman, Nicht Kursiv
Formatiert: Schriftart: Nicht Kursiv

show how significant the effect of the residual dose may be in ESR dating of fluvial sediments.

Dose recovery test

A dose recovery test, using the SAR protocol, was performed for all four ESR signals by adding 963 Gy on top of the natural signal using three aliquots of sample RB-II and thus is considered to be a new "natural" signal. The test was used to check the accuracy of the measurement protocol because the thermal treatment included in the SAR protocol may change sensitivity of the ESR centres ~~per unit dose~~. The D_e values of the aliquots (natural + 963 Gy) were measured by the SAR protocol, with 3 dose steps up to 3516 Gy. The dose recovery ratio was calculated by subtracting the natural D_e from the recovered dose and the difference of the natural + 963 Gy and the natural D_e was then divided by the added dose of 963 Gy. This experiment is a modified version of the single aliquot regenerative and added dose (SARA) by Tsukamoto et al. (2017) with a single added dose point. The dose recovery results (cf. Fig. 4) are ~~satisfying~~ satisfactory for the Ti-Li and Ti-mix signal with a ratio of 0.98 ± 0.07 and 1.00 ± 0.15, respectively, indicating that ESR SAR protocol works well for these signals. Our results resemble the results published by (Tsukamoto et al., 2017). The dose recovery ratio for the Al signal is high with 1.75 ± 0.18, ~~which indicates a sensitivity change due to thermal treatment during SAR protocol, therefore the reported residual doses may be overestimated. The dose recovery~~whereas the ratio of the Ti-H signal is low (0.55 ± 0.17). The significantly smaller Ti-H D_e compared to the Ti-Li D_e is probably partly a result of this (underestimating). The result of our dose recovery test suggests that the applied SAR protocol is robust in the dose estimation for the Ti-Li and Ti-mix signals, whereas those from the Al and Ti-H centres could be over- and underestimated.

5 Discussion and conclusion

The results clearly show that the ESR D_e for all samples are significantly larger than the OSL D_e of Lauer et al. (2011) and therefore residual subtraction is highly recommended if a representative modern analogue sample is available. Furthermore, the observed residual doses ~~confirm~~ follow the trend in the signal's bleaching behaviour as described by Toyoda et al. (2000): the Al centre shows the largest residual followed by the Ti-Li and Ti-H with the lowest. The size of the residual dose for the Ti-mix lies in between the Ti-Li and Ti-H. However, it should be noted that the recovered dose in the dose recovery test overestimated the given dose for the Al centre and showed underestimation for the Ti-H centre, which may have influenced the observed residual dose. Although the Ti-H shows the smallest D_e, hence is closest to the expected OSL D_e, it is unreliable because it failed to recover the known given dose.

Formatiert: Schriftart: Times New Roman, Nicht Kursiv

Formatiert: Schriftart: Times New Roman, Nicht Kursiv

Formatiert: Schriftart: Times New Roman, Nicht Kursiv

Formatiert: Schriftart: Times New Roman, Nicht Kursiv

Formatiert: Schriftart: Times New Roman, Nicht Kursiv

Formatiert: Schriftart: Times New Roman, Nicht Kursiv

Formatiert: Schriftart: Times New Roman, Nicht Kursiv

Formatiert: Schriftart: Times New Roman, Nicht Kursiv

Formatiert: Schriftart: Times New Roman, Nicht Kursiv

~~-~~Regarding the Al centre, we did not estimate the size of the bleachable/unbleachable components by a bleaching test. Instead, a measured residual dose from young samples, preferably obtained from the same set of sedimentary sequence could be subtracted from the D_e of older samples; this approach has an advantage over the very time consuming bleaching experiment with the solar simulator for ~1000 hours. Fig. 5 shows a comparison of all residual doses for the Al and Ti-Li. Additionally a linear fitting was performed yielding the y-intercept of 90 ± 220 Gy. This intercept indicates a rough estimate of the size of residual dose for the unbleachable Al centre, although it ~~does not agree with~~is much smaller than the values reported by Tsukamoto et al. (2018) and Timar-Gabor et al. (2020) from aeolian sediments.~~.~~

However, the result of the dose recovery test suggests that ~~the ratio of bleachable/unbleachable components should be compared before and after the annealing step, in order to understand the problem of the dose recovery test~~the thermal annealing step in the SAR protocol changed the signal production efficiency of the Al centre. We hypothesise that the annealing changed the ratio of bleachable/unbleachable components of the Al centre, which led to the failure of the dose recovery test. Timar-Gabor et al. (2020) demonstrated that the intensity of both bleachable and unbleachable Al centre can be increased by additive dose irradiation on natural aliquots. They explained that the Al centre has an unbleachable component, because the amount of Al in quartz is far more abundant compared to any other electron centres, which contribute bleaching (and recombine with the Al-hole centre). ~~-~~However, a thermal annealing reset both populations, and following irradiation may have only produced the bleachable Al centre.~~-~~ Although this hypothesis must be tested experimentally, a supporting evidence of the hypothesis is available from a comparison of the natural and regenerative dose response curves of the Al centre from the Chinese Loess Plateau. Tsukamoto et al. (2018) showed that the regenerated dose response curve, which was constructed after an annealing, was only comparable to the natural one, when the unbleachable Al signal intensity was subtracted from the natural dose response curve, suggesting that the regenerative dose response curve was dominated by the bleachable Al centre.

~~Fig. 5 shows a comparison of all residual doses for the Al and Ti-Li. Additionally a linear fitting was performed yielding the y-intercept of 90 ± 220 Gy. This intercept indicates a rough estimate of the size of residual dose for the unbleachable Al centre, although this never replaces a proper bleaching test to estimate the unbleachable signal component.~~

The dose recovery test of the Ti centre indicates that Ti-Li centre does not suffer any sensitivity changes after the annealing, whereas the Ti-H centre underestimates the given dose significantly. Beerten and Stesmans (2006) reported strong deviations in Ti-Li and Ti-H SAR D_e from the expected dose, although the total Ti centre provided a reliable result. They suggested different possible explanations including 1) charge transfer between Ti-Li and Ti-H centres during the artificial irradiation and ~~, 2) a thermal fading of the Ti-H centre, and 3~~2) differences in production efficiency but eventually leaving the question open. Similar problems might have also affected the

Formatiert: Einzug: Erste Zeile: 1,08 cm

Formatiert: Tiefgestellt

Formatiert: Schriftart: 10 Pt.

Formatiert: Einzug: Erste Zeile: 1,08 cm observed difference in the dose recovery ratios of the different Ti signals. More effort is needed to fully understand about the behaviour of different Ti signals.

Though there is only little available sedimentological information from the sampling locationsfor the samples is limited, we triedcompared the observed residual dose in to see if the different fluvial depositional environments and their different bleaching kinetics reflectaffected in the residual dose size. From Lauer et al. (, 2011), we identified three different depositional environments, which include i) overbank deposits, ii) deposits from braided river systems and iii) deposits of a channel, meansi.e., meandering river system (personal communication with Dr. Michael Kenzler). The Rheinberg samples (RB-II and I) were taken from a point bar setting and have been interpreted as channel deposits of a meandering river. The samples from Monheim-Hitdorf seem to bewere deposited in a braided river system with channel- and sheetflow deposits. At Libur, sample LB-I seems to be takenoriginated from a braided river system. Niederkassel site sample NK-I was deposited in a braided river system, whereas the lower NK-II sample seem to originate from an overbank deposit. The Aloysiushof/Dormagen sample (ALH-III) stems from the uppermost gravel rich part of the profile and probably channel deposit.

Only from this information, it is still rather difficult to tell about the bleaching kinetics of the different fluvial environments. Probably, the overbank deposits could have experienced the poorest bleaching, as one could expect a higher suspension load within the water. From the ESR residual doses, we do not see this as sample NK-II, which was identified as an overbank deposit shows relatively small residual doses compared to the rest of the samples. In generalFrom the observed residual doses, we do not see any pattern at all which links a certain depositional environment to especially good or bad bleaching kinetics in our set of samplesaccording to different depositional environments. Instead, all residual doses for our samples are relatively uniform, with a mean of 1270 ± 120 Gy for the Al centre (including the unbleachable signal partcomponent), 591 ± 53 Gy for the Ti-Li centre, 170 ± 21 Gy for the Ti-H), and 470 ± 42 Gy for the Ti-mix..

. The residual dose for the unbleachable Al centre is roughly consistent with the observation of Tsukamoto et al. (2018) from Chinese loess (~500 Gy) and of Timar-Gabor et al. (2020) for the various aeolian sediments (~500-700 Gy) from the Al centre. Beerten and Stesmans (2006) reported strong deviations in Ti-Li and Ti-H D_e from the expected dose which led to a discussion to explain this offset in doses. In our case the dose recovery test indicates that Ti-Li centre does not suffer any sensitivity changes whereas the Ti-H centre underestimates the given dose significantly. Beerten and Stesmans (2006) suggested several possibilities to explain this phenomenon. These included 1) charge transfer between Ti-Li and Ti-H centres during the artificial irradiation, 2) a thermal fading of the Ti-H centre, and 3) differences in production efficiency but eventually leaving the question open. More effort is needed to fully understand this issue. Moreover, we propose conducting a modified version of the here used SAR protocol in which the thermal annealing step is replaced by optical depletion of the natural signal in order to achieve a better dose recovery behaviour for especially the Al centre and Ti-H centre. In conclusion, we show that all of the

Formatiert: Einzug: Erste Zeile: 1,08 cm

Formatiert: Einzug: Erste Zeile: 1,08 cm

Formatiert: Einzug: Erste Zeile: 1,08 cm

Formatiert: Tiefgestellt

investigated fluvial sediments were not fully bleached before burial and after subtraction of OSL D_e still a significant amount of residual dose is carried by the samples. Even the Ti-H, which is supposed to be best bleachable, is far from zero. This highlights the importance of further-investigation into the dynamics of residual doses in both, aeolian and fluvial environments.

Formatiert: Tiefgestellt

Data availability. All data generated or analysed during this study are included in this published article.

Formatiert: Block

Author contributions. MR and ST conceived the study, MR carried out the measurements with input from ST. MR wrote the paper with input from ST.

Formatiert: Block

Competing interests. Sumiko Tsukamoto declares a conflict of interest, as she is an Associate Editor forof GeochronologyThe authors declare that they have no conflict of interest.

Formatiert: Block

Acknowledgements. We are grateful to Gwynlyn Buchanan for language corrections sand . Michael Kenzler for sedimentological interpretation. The constructive comments from two three reviewers, Mathieu Duval and twoan anonymous reviewers, helped to improve the paper.

References

Asagoe, M., Toyoda, S., Voinchet, P., Falguères, C., Tissoux, H., Suzuki, T., and Banerjee, D.: ESR dating of tephra with dose recovery test for impurity centers in quartz, Quaternary International, 246, 118–123, https://doi.org/10.1016/j.quaint.2011.06.027, http://www.sciencedirect.com/science/article/pii/S1040618211003466, 2011.

Bahain, J.-J., Falguères, C., Laurent, M., Voinchet, P., Dolo, J.-M., Antoine, P., and Tuffreau, A.: ESR chronology of the Somme River Terrace system and first human settlements in Northern France, Quaternary Geochronology, 2, 356–362, https://doi.org/10.1016/j.quageo.2006.04.012, https://linkinghub.elsevier.com/retrieve/pii/S1871101406000276, 2007.

Bartz, M., Rixhon, G., Duval, M., King, G. E., Álvarez Posada, C., Parés, J. M., and Brückner, H.: Successful combination of electron spin resonance, luminescence and palaeomagnetic dating methods allows reconstruction of the Pleistocene evolution of the lower Moulouya river (NE Morocco), Quaternary Science Reviews, 185, 153–171, https://doi.org/10.1016/j.quascirev.2017.11.008, https://linkinghub.elsevier.com/retrieve/pii/S0277379117305474, 2018.

Bartz, M., Arnold, L., Demuro, M., Duval, M., King, G., Rixhon, G., Álvarez Posada, C., Parés, J., and Brückner, H.: Single-grain TT-OSL dating results confirm an Early Pleistocene age for the lower Moulouya River deposits (NE Morocco), Quaternary Geochronology, 49, 138–145, https://doi.org/https://doi.org/10.1016/j.quageo.2018.04.007, https://www.sciencedirect.com/science/article/pii/S1871101417302121, 15th International Conference on Luminescence and Electron Spin Resonance Dating, 11-15 September 2017, Cape Town, South Africa, 2019.

Bartz, M., Duval, M., Brill, D., Zander, A., King, G. E., Rhein, A., Walk, J., Stauch, G., Lehmkuhl, F., and Brückner, H.: Testing the potential of K-feldspar pIR-IRSL and quartz ESR for dating coastal alluvial fan complexes in arid environments, Quaternary International, 556, 124–143, https://doi.org/10.1016/j.quaint.2020.03.037, http://www.sciencedirect.com/science/article/pii/S1040618220301300, 2020.

Beerten, K. and Stesmans, A.: The use of Ti centers for estimating burial doses of single quartz grains: A case study from an aeolian deposit Ma old, Radiation Measurements, 41, 418–424, https://doi.org/10.1016/j.radmeas.2005.10.004, https://linkinghub.elsevier.com/retrieve/ pii/S1350448705002763, 2006.

Beerten, K., Lomax, J., Clémer, K., Stesmans, A., and Radtke, U.: On the use of Ti centres for estimating burial ages of Pleistocene sedimentary quartz: Multiple-grain data from Australia, Quaternary Geochronology, 1, 151–158, https://doi.org/10.1016/j.quageo.2006.05.037, https://linkinghub.elsevier.com/retrieve/pii/S1871101406000690, 2006.

Beerten, K., Rittner, S., Lomax, J., and Radtke, U.: Dose recovery tests using Ti-related ESR signals in quartz: First results, Quaternary Geochronology, 3, 143–149, https://doi.org/10.1016/j.quageo.2007.05.002, https://linkinghub.elsevier.com/retrieve/pii/ S1871101407000398, 2008.

Beerten, K., Verbeeck, K., Laloy, E., Vanacker, V., Vandenberghe, D., Christl, M., De Grave, J., and Wouters, L.: Electron spin resonance (ESR), optically stimulated luminescence (OSL) and terrestrial cosmogenic radionuclide (TCN) dating of quartz from a Plio-Pleistocene sandy formation in the Campine area, NE Belgium, Quaternary International, 556, 144–158, https://doi.org/10.1016/j.quaint.2020.06.011, http://www.sciencedirect.com/science/article/pii/S1040618220303232, 2020.

del Val, M., Duval, M., Medialdea, A., Bateman, M. D., Moreno, D., Arriolabengoa, M., Aranburu, A., and Iriarte, E.: First chronostratigraphic framework of fluvial terrace systems in the eastern Cantabrian margin (Bay of Biscay, Spain), Quaternary Geochronology, 49, 108–114, https://doi.org/10.1016/j.quageo.2018.07.001, https://linkinghub.elsevier.com/retrieve/pii/S1871101417302546, 2019.

Duval, M. and Guilarte, V.: ESR dosimetry of optically bleached quartz grains extracted from Plio-Quaternary sediment: Evaluating some key aspects of the ESR signals associated to the Ti-centers, Radiation Measurements, 78, 28–41, https://doi.org/10.1016/j.radmeas.2014.10.002, ~~https://linkinghub.elsevier.com/retrieve/pii/S1350448714002741,~~ 2015.

Duval, M., Sancho, C., Calle, M., Guilarte, V., and Peña-Monné, J. L.: On the interest of using the multiple center approach in ESR dating of optically bleached quartz grains: Some examples from the Early Pleistocene terraces of the Alcanadre River (Ebro basin, Spain), Quaternary Geochronology, 29, 58–69, https://doi.org/10.1016/j.quageo.2015.06.006, ~~https://linkinghub.elsevier.com/retrieve/pii/ S1871101415300418,~~ 2015.

Duval, M., Arnold, L. J., Guilarte, V., Demuro, M., Santonja, M., and Pérez-González, A.: Electron spin resonance dating of optically bleached quartz grains from the Middle Palaeolithic site of Cuesta de la Bajada (Spain) using the multiple centres approach, Quaternary Geochronology, 37, 82–96, https://doi.org/10.1016/j.quageo.2016.09.006, ~~http://www.sciencedirect.com/science/article/pii/S1871101416300759,~~ 2017.

Duval, M., Voinchet, P., Arnold, L. J., Parés, J. M., Minnella, W., Guilarte, V., Demuro, M., Falguères, C., Bahain, J.-J., and Despriée, J.: A multi-technique dating study of two Lower Palaeolithic sites from the Cher Valley (Middle Loire Catchment, France): Lunery-la Terre-des-Sablons and Brinay-la Noira, Quaternary International, 556, 71–87, https://doi.org/10.1016/j.quaint.2020.05.033, ~~http://www. sciencedirect.com/science/article/pii/S1040618220302664,~~ 2020.

Fang, F. and Grün, R.: ESR thermochronometry of Al and Ti centres in quartz: A case study of the Fergusons Hill-1 borehole from the Otway Basin, Australia, Radiation Measurements, 139, 106 447, https://doi.org/10.1016/j.radmeas.2020.106447, 2020.

Frechen, M.: Systematic thermoluminescence dating of two loess profiles from the Middle Rhine Area (F.R.G.), Quaternary Science Reviews, 11, 93–101, https://doi.org/10.1016/0277-3791(92)90048-D, ~~http://www.sciencedirect.com/science/article/pii/027737919290048D,~~ 1992.

Kars, R. H., Reimann, T., and Wallinga, J.: Are feldspar SAR protocols appropriate for post-IR IRSL dating?, Quaternary Geochronology, 22, 126–136, https://doi.org/10.1016/j.quageo.2014.04.001, ~~http://www.sciencedirect.com/science/article/pii/S1871101414000326,~~ 2014.

Lauer, T., Frechen, M., Klostermann, J., Krbetschek, M., Schollmayer, G., and Tsukamoto, S.: Luminescence dating of Last Glacial and Early Holocene fluvial deposits from the Lower Rhine methodological aspects and chronological framework, Zeitschrift der Deutschen Gesellschaft für Geowissenschaften, pp. 47–61, https://doi.org/10.1127/1860-1804/2011/0162-0047, ~~https://www.schweizerbart.de/papers/zdgg/detail/162/75689/Luminescence_dating_of_Last_Glacial_and_Early_Holocene_fluvial_ deposits_from_the_Lower_Rhine_methodological_aspects_and_chronological_framework,~~ 2011.

Laurent, M., Falguères, C., Bahain, J., Rousseau, L., and Van Vliet Lanoé, B.: ESR dating of quartz extracted from quaternary and neogene sediments__method, potential and actual limits, Quaternary Science Reviews, 17, 1057–1062, https://doi.org/10.1016/S0277- 3791(97)00101-7, ~~https://linkinghub.elsevier.com/retrieve/pii/S0277379197001017,~~ 1998.

Mejdahl, V. and Bøtter-Jensen, L.: Luminescence dating of archaeological materials using a new technique based on single aliquot measurements, Quaternary Science Reviews, 13, 551–554, https://doi.org/10.1016/0277-3791(94)90076-0, ~~http://www.sciencedirect.com/science/ article/pii/0277379194900760,~~ 1994.

Murray, A. S. and Wintle, A. G.: The single aliquot regenerative dose protocol: potential for improvements in reliability, Radiation Measurements, 37, 377–381, https://doi.org/10.1016/S1350-4487(03)00053-2, ~~https://www.sciencedirect.com/science/article/pii/S1350448703000532,~~ 2003.

Oppermann, F. and Tsukamoto, S.: A portable system of X-ray irradiation and heating for electron spin resonance (ESR) dating, Ancient TL, 33, 11–15, 2015.

Richter, M., Tsukamoto, S., and Long, H.: ESR dating of Chinese loess using the quartz Ti centre: A comparison with independent age con~~-~~trol, Quaternary International, 556, 159–164, https://doi.org/10.1016/j.quaint.2019.04.003, ~~http://www.sciencedirect.com/science/article/ pii/S1040618218308450,~~ 2020.

Rink, W., Bartoll, J., Schwarcz, H., Shane, P., and Bar-Yosef, O.: Testing the reliability of ESR dating of optically exposed buried quartz sedi~~-~~ments, Radiation Measurements, 42, 1618–1626, https://doi.org/10.1016/j.radmeas.2007.09.005, ~~https://linkinghub.elsevier.com/retrieve/ pii/S1350448707003769,~~ 2007.

Timar-Gabor, A., Chruścińska, A., Benzid, K., Fitzsimmons, K., Begy, R., and Bailey, M.: Bleaching studies on Al~~-~~hole ([AlO4/h]0) electron spin resonance (ESR) signal in sedimentary quartz, Radiation Measurements, 130, 106 221, https://doi.org/10.1016/j.radmeas.2019.106221, ~~https://linkinghub.elsevier.com/retrieve/pii/S1350448719305074,~~ 2020.

Tissoux, H., Falguères, C., Voinchet, P., Toyoda, S., Bahain, J., and Despriée, J.: Potential use of Ti-center in ESR dating of fluvial sedi~~-~~ment, Quaternary Geochronology, 2, 367–372, https://doi.org/10.1016/j.quageo.2006.04.006, ~~https://linkinghub.elsevier.com/retrieve/pii/ S1871101406000239,~~ 2007.

Tissoux, H., Toyoda, S., Falguères, C., Voinchet, P., Takada, M., Bahain, J.-J., and Despriée, J.: ESR Dating of Sedimentary Quartz from Two Pleistocene Deposits Using Al and Ti-Centers, Geochronometria, 30, 23–31, https://doi.org/10.2478/v10003-008-0004-y, ~~https://content. sciendo.com/doi/10.2478/v10003-008-0004-y,~~ 2008.

Toyoda, S. and Falguères, C.: The method to represent the ESR signal intensity of the aluminium hole center in quartz for the purpose of dating, Advances in ESR applications, pp. 7–10, 2003.

Toyoda, S., Voinchet, P., Falguères, C., Dolo, J. M., and Laurent, M.: Bleaching of ESR signals by the sunlight: a laboratory experiment for establishing the ESR dating of sediments, Applied Radiation and Isotopes, 52, 1357–1362, https://doi.org/10.1016/S0969-8043(00)00095-~~-~~6, ~~https://linkinghub.elsevier.com/retrieve/pii/S0969804300000956,~~ 2000.

Toyoda, S., Miura, H., and Tissoux, H.: Signal regeneration in ESR dating of tephra with quartz, Radiation Measurements, 44, 483–487, https://doi.org/10.1016/j.radmeas.2009.03.002, proceedings of the 12th International Conference on Luminescence and Electron Spin Resonance Dating (LED 2008), 2009.

Tsukamoto, S., Toyoda, S., Tani, A., and Oppermann, F.: Single aliquot regenerative dose method for ESR dating using X-ray irradiation and preheat, Radiation Measurements, 81, 9–15, https://doi.org/10.1016/j.radmeas.2015.01.018, ~~http://www.sciencedirect.com/science/ article/pii/S1350448715000268,~~ 2015.

Tsukamoto, S., Porat, N., and Ankjærgaard, C.: Dose recovery and residual dose of quartz ESR signals using modern sediments: Implications for single aliquot ESR dating, Radiation Measurements, 106, 472–476, https://doi.org/10.1016/j.radmeas.2017.02.010, ~~http://www.sciencedirect.com/science/article/pii/S1350448717301087,~~ 2017.

Tsukamoto, S., Long, H., Richter, M., Li, Y., King, G. E., He, Z., Yang, L., Zhang, J., and Lambert, R.: Quartz natural and laboratory ESR dose response curves: A first attempt from Chinese loess, Radiation Measurements, 120, 137–142, https://doi.org/10.1016/j.radmeas.2018.09.008, http://www.sciencedirect.com/science/article/pii/S1350448717308016, 2018.

Tsukamoto, S., Oppermann, F., Autzen, M., Richter, M., Bailey, M., Ankjærgaard, C., and Jain, M.: Response of the Ti and Al electron spin resonance signals in quartz to X-ray irradiation, Radiation MeasurementsRadiation Measurements, 149, 106676, https://doi.org/10.1016/j.radmeas.2021.106676, 2021., submitted.

Voinchet, P., Falguères, C., Laurent, M., Toyoda, S., Bahain, J., and Dolo, J.: Artificial optical bleaching of the Aluminium center in quartz implications to ESR dating of sediments, Quaternary Science Reviews, 22, 1335–1338, https://doi.org/10.1016/S0277-3791(03)00062-3, https://linkinghub.elsevier.com/retrieve/pii/S0277379103000623, 2003.

Voinchet, P., Toyoda, S., Falguères, C., Hernandez, M., Tissoux, H., Moreno, D., and Bahain, J.-J.: Evaluation of ESR resid-ual dose in quartz modern samples, an investigation on environmental dependence, Quaternary Geochronology, 30, 506–512, https://doi.org/10.1016/j.quageo.2015.02.017, https://linkinghub.elsevier.com/retrieve/pii/S1871101415000308, 2015.

Voinchet, P., Yin, G., Falguères, C., Liu, C., Han, F., Sun, X., and Bahain, J.-J.: Dating of the stepped quaternary fluvial terrace system of the Yellow River by electron spin resonance (ESR), Quaternary Geochronology, 49, 278–282, https://doi.org/10.1016/j.quageo.2018.08.001, https://linkinghub.elsevier.com/retrieve/pii/S1871101417302091, 2019.

Yokoyama, Y., Falgueres, C., and Quaegebeur, J.: ESR dating of quartz from quaternary sediments: First attempt, Nuclear Tracks and Radiation Measurements, 10, 921–928, https://doi.org/10.1016/0735-245X(85)90109-7, https://linkinghub.elsevier.com/retrieve/pii/ 0735245X85901097, 1985.

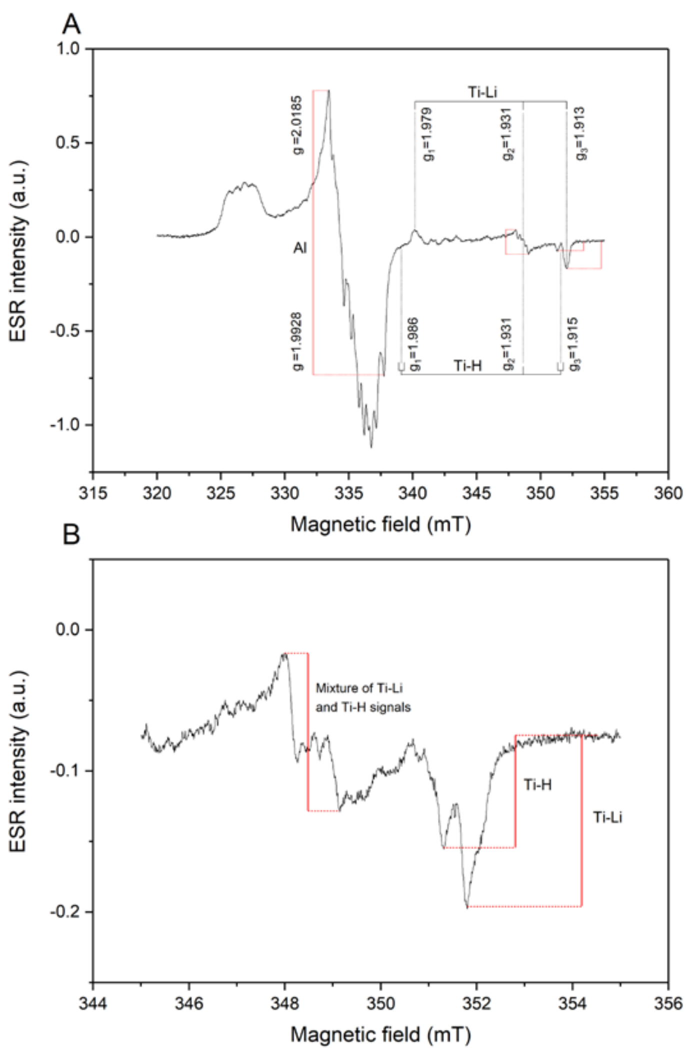

Figure 1. A) The natural Al centre and Ti centres of sample RB-II and overview of the g-values; B) Close-up of Titanium signals of sample RB-II after annealing and giving 500 Gy of artificial irradiation.

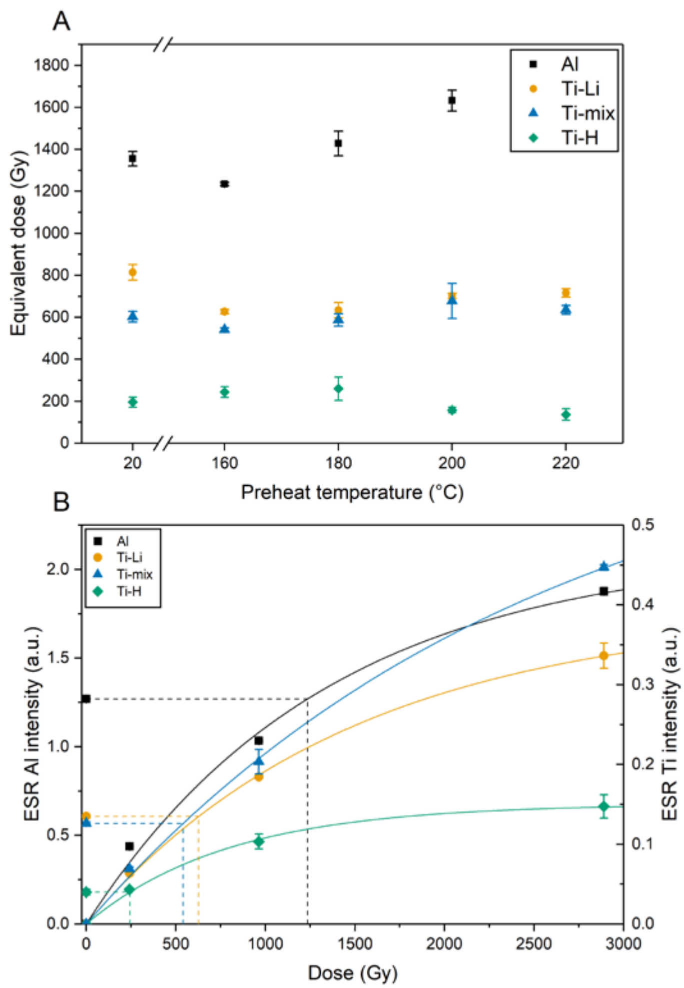

Figure 2. A) Preheat plateau test for sSample RB-II. The dose response curve for Al centre for 220 °C did not fit, so the D_e value was not obtained. B) Dashed lines indicate the mean dose for each signal. B) The DRC's for 160 °C preheat temperature for each one of the ESR centres. The D_e are marked.

Formatiert: Schriftart: Times New Roman, Nicht Kursiv

Formatiert: Schriftart: Times New Roman, Nicht Kursiv

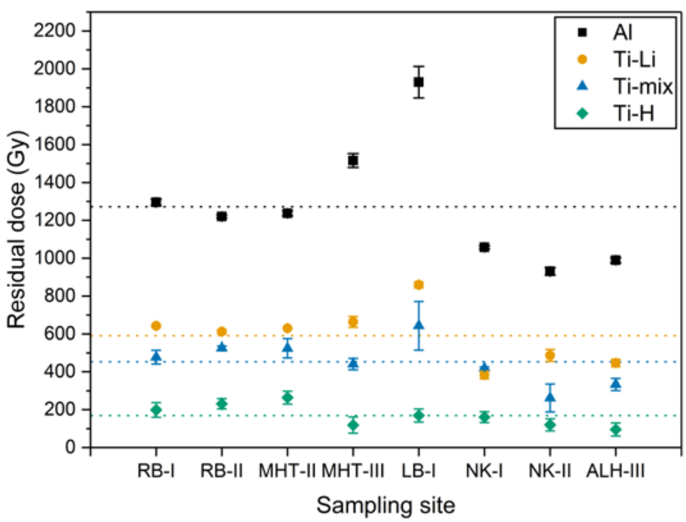

Figure 3. Residual doses of the four different ESR signals for all samples. Dotted lines indicate the mean dose for each signal.

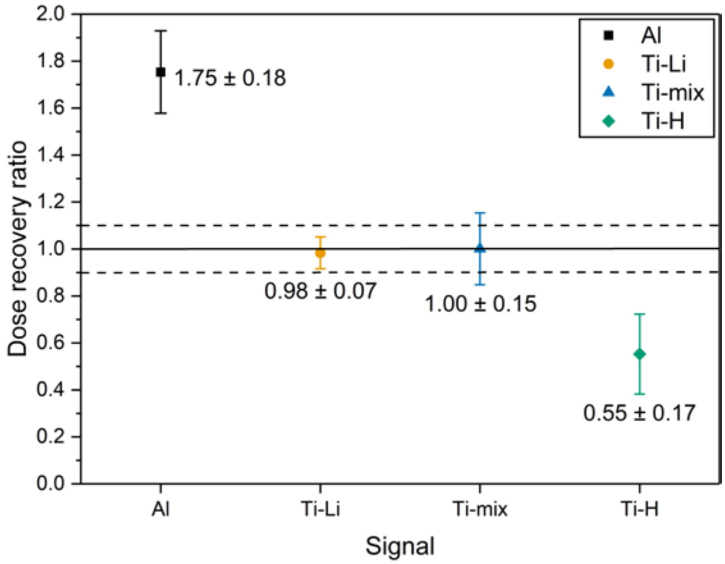

Figure 4. Dose recovery ratios. The dashed lines mark the 10% deviation margin.

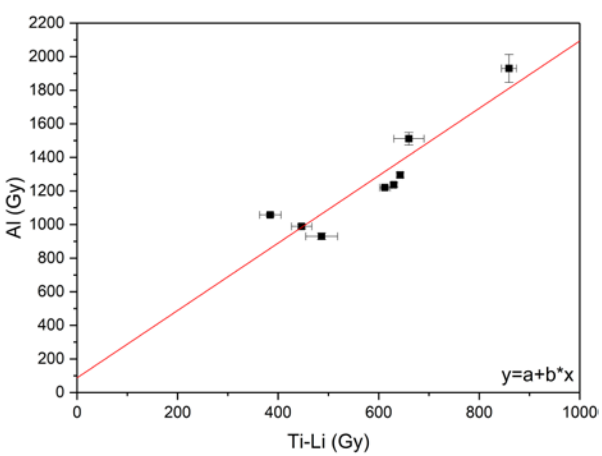

Figure 5. Comparison of ESR Al and Ti-Li residual doses with linear fitting.

Table 1. Sample description after (Lauer et al., 2011).Lauer et al. (2011).

Sample ID	Description
RB-I	cross-bedded sand with small amounts of Laacher See Tephra
RB-II	horizontally laminated, well sorted fluvial sand
MHT-II	horizontally laminated sand
MHT-III	horizontally laminated sand
LB-I	horizontally layered sand
NK-I	cross-bedded sand layers
NK-II	overbank deposits
ALH-III	fluvial sand, more gravel-rich with clay clasts

Formatiert: Schriftart: 9 Pt.

Formatiert: Schriftart: 9 Pt.

Formatiert: Schriftart: 9 Pt.

Table 2. Mean ESR equivalent doses (D_e) and residual doses of the 4 signals compared with the mean OSL D_e.

Sample ID	Equivalent dose				Residual dose				
	Al* (Gy)	Ti-Li (Gy)	Ti-mix (Gy)	Ti-H (Gy)	Al* (Gy)	Ti-Li (Gy)	Ti-mix (Gy)	Ti-H (Gy)	OSL** (Gy)
RB-I	1364 1314 ± 1716	686 661 ± 5	515 496 ± 536	21725 ± 4039	1296346 ± 17	64368 ± 5	47896 ± 368	199207 ± 3940	18.4 ± 0.4
RB-II	123582 ± 8	62751 ± 1001	54061 ± 1001	24655 ± 278	122067 ± 8	612636 ± 11	52646 ± 11	23140 ± 278	14.8 ± 0.3
MHT-I	1602 ± 37	718 ± 29	486 ± 31	151 ± 44	1571 ± 39	686 ± 31	454 ± 32	120 ± 46	31.2 ± 1.9
MHT-II	1266315 ± 12	65984 ± 2	55374 ± 520	292304 ± 334	123786 ± 134	63055 ± 3	52446 ± 513	26475 ± 3634	28.8 ± 1.3
MHT-III	1543 ± 37	691 ± 28	468 ± 29	146 ± 42	1516 ± 37	664 ± 29	441 ± 30	119 ± 43	27.0 ± 0.8
LB-I	20196338 ± 825	893927 ± 134	677703 ± 132127	2021 ± 335	19302005 ± 836	85993 ± 15	64369 ± 112934	16977 ± 356	33.3 ± 1.4
NK-I	1086128 ± 6	41329 ± 1920	44865 ± 5	18997 ± 278	105799 ± 8	384400 ± 212	41936 ± 7	1608 ± 2930	28.9 ± 2.0
NK-II	96197 ± 189	51736 ± 312	292303 ± 7573	1505 ± 312	93167 ± 1920	487506 ± 323	26273 ± 746	1205 ± 323	30.0 ± 1.0
ALH-III	100948 ± 13	485 467 ± 2019	35367 ± 312	11520 ± 3335	9891028 ± 14	464475 ± 201	33347 ± 323	95100 ± 356	20.1 ± 1.2

* including unbleachable signal component

** Lauer et al. (2011)

Table 3. External dose rates, ESR ages derived from D_e, residual ages before burial and mean OSL ages for comparison.

Sample ID	Ext. dose rate*	Age (from D_e)				Residual age before burial				
	Gy/ka	Al** (ka)	Ti-Li (ka)	Ti-mix (ka)	Ti-H (ka)	Al* (ka)	Ti-Li (ka)	Ti-mix (ka)	Ti-H (ka)	OSL (ka)
RB-I	2.15±0.11	611±32 ~~635±33~~	308±16 ~~319±16~~	231±21 ~~239±21~~	101±19 ~~105±19~~	603±32 ~~626±33~~	299±15 ~~311±16~~	222±20 ~~231±21~~	92±19 ~~96±19~~	8.6 ± 0.5
RB-II	1.67±0.08	739±36 ~~768±37~~	375±19 ~~390±20~~	324±17 ~~336±17~~	147±18 ~~153±18~~	731±35 ~~759±37~~	367±19 ~~381±19~~	315±16 ~~327±17~~	138±18 ~~144±18~~	8.9 ± 0.5

Formatiert: Sch
Formatiert
Formatiert
Formatiert
Formatiert: Sch
Formatiert
Formatiert
Formatiert
Formatiert
Formatiert
Formatiert
Formatiert
Formatiert
Formatiert: Sch
Formatiert: Sch
Formatiert
Formatiert
Formatiert
Formatiert
Formatiert
Formatiert
Formatiert
Formatiert
Formatiert: Sch

MHT-II	2.41±0.182.57 ±0.27	525± 40623±67	273± 20279±31	230± 27189±23	121± 1659±18	513± 39611±66	261± 20267±31	218± 27177±22	109± 1647±19	12.01 ± 1.50
MHT-III	2.28±0.262.4 1±0.18	677± 79545±41	303± 37284±21	205± 27238±28	64± 20126±17	665± 77533±40	291± 36272±20	193± 26226±28	52± 20114±17	112.80 ± 1.40
LB-I	2.08±0.15	944± 79980±82	429± 32446±33	325± 66338±68	97± 17101±18	928± 78964±81	413± 31430±32	309± 66322±68	81± 1885±18	16.0 ± 1.3
NK-I	2.01±0.10	540± 27561±28	206± 14213±15	223± 11231±12	94± 1498±15	526± 26547±28	191± 14199±15	209± 11217±11	80± 1583±15	14.4 ± 1.2
NK-II	2.11±0.12	455± 27473±28	245± 20254±21	138± 35144±37	71± 1574±16	441± 27458±28	231± 20240±21	124± 36129±37	57± 1559±16	14.2 ± 0.9
ALH-III	1.48±0.15	682± 70708±72	315± 34327±36	239± 32243±33	78± 2481±25	668± 68694±71	302± 33314±35	225± 32234±33	64± 2467±25	13.6 ± 1.6

* Lauer et al. (2011)

** including unbleachable signal component

Table 4. ESR SAR protocol modified after Tsukamoto et al. (2015).

Step	Treatment
1	Preheat (T °C for 4 minutes)[a]
2	Natural ESR
3	Anneal (300 °C for 120 minutes)
4	ESR after annealing
5	Artificial irradiation
6	Preheat (T °C for 4 minutes)[a]
7	Regenerated ESR
8	Repeat 5-7

[a] T is preheat temperature in degree centigrade

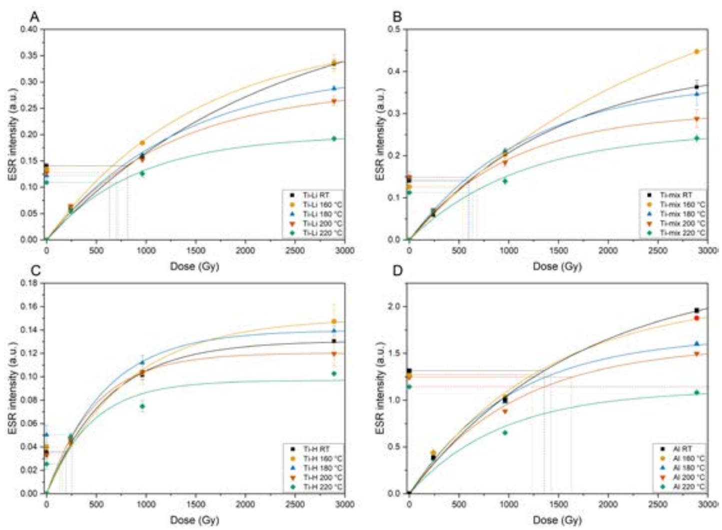

Figure A1. The DRC's for each preheat temperature (RT = room temperature = 20 °C) for each one of the ESR centres. The D_e are marked.

Formatiert: Schriftart: Fett

Formatiert: Tiefgestellt